

Kinethical Aspects of High Solid Contents Copoly(Styrene/Butylacrylate)-Cloisite 30B Nanocomposites

M. Mirzataheri

Iran Polymer & Petrochemical Institute, P. O. Box. 14965/115, Tehran, Iran

Article history:

Received 26/12/2013

Accepted 13/2/2014

Published online 1/3/2014

Keywords:

High solid content

Kinetics

Cloisite 30B

Rate of polymerization

**Corresponding author:*

E-mail address:

m.mirzataheri@ippi.ac.ir

Phone: 98 912 1893 880

Fax: +98 21 44580023

Abstract

High solid content poly (styrene-co-butyl acrylate) latex (with 20% and 40% solid content) including high amounts of Cloisite 30B (7 wt% and 10 wt%) were kinetically investigated. Gravimetric method via measuring the rate of polymerization, number of particles and average number of radicals per particle was used. Results showed that by increasing the solid content; the average diameter of polymer particles decreased. Studies on the polymerization rate depict that the increase in polymer particle size provides more average reactive radicals per polymer particle, which increased from 0.48 to 0.88 for the sample containing 7 wt% clay and 20 wt% solid content. Observed armored particles with honeycomb morphology is the most novelty of this research work, which is suitable for making barrier packaging films.

2014 JNS All rights reserved

1. Introduction

Miniemulsion technique is almost a new technique of polymerization, which is formed by ultrasonication homogenization of emulsion through droplet nucleation mechanism within the polymerization reaction [1-3]. In a real miniemulsion, monomer droplets should strongly be stabilized against two destructive processes. These destructive processes are Ostwald ripening degradation (τ_1 mechanism) and coalescence degradation (τ_2 mechanism) [4-6]. Latex instability which happens by these unexpected two processes has unfavorable effects on the number of monomer

droplets, rate of polymerization and polymer particle size [7-9]. For this purpose, hydrophobic materials are introduced in order to produce virtual osmotic pressure for restricting the monomer migration from the monomer droplets. In miniemulsion, as the surfactant concentration is kept below the critical micelle concentration (CMC); nucleation occurs primarily within the monomer droplets and not as micellar nucleation. This phenomenon eliminates micellar and homogeneous nucleations [7, 10-11]. Also, ionic or nonionic surfactants are used to provide the droplets with colloidal stability against coalescence

[7]. Dungen and coworkers used Pickering miniemulsion of (styrene-co-butyl acrylate) and believed their latexes were more stable than SDS stabilized latexes; however other nanomaterials had strange effects on the mechanism of polymerization [12].

Effect of nanoclay on the kinetics of atom transfer radical bulk homo and copolymerization of styrene and methyl methacrylate (MMA) initiated with CCl_3 -terminated poly (vinyl acetate) was investigated when $\text{CuCl}/\text{PMDETA}$ was used as a catalyst system. Results showed that nanoclay significantly enhances the homopolymerization rate of MMA [13].

Montmorillonite ion-exchanged with a mixed classical and double bond containing modifier was used to synthesize well-defined poly (styrene-co-butyl acrylate) nanocomposites via AGET ATRP. Clay-attached poly (styrene-co-butyl acrylate) chains demonstrated a higher molecular weight and lower PDI in comparison with the free copolymer chains. Partially exfoliated morphology of clay layers obtained for low clay loading nanocomposites [14]. Considering the linear first-order kinetics of the polymerization, AGET and normal atom transfer radical polymerization (ATRP) in the presence of clay nanolayers were carried out. The linearity of $\ln([M]_0/[M])$ versus time and also molecular weight distribution against conversion, indicated that the proportion of propagating radicals is almost constant during the polymerization, which was the result of contribution of termination and transfer reactions [15].

Poly (styrene-co-butyl acrylate)/clay nanocomposites were synthesized via activators generated by electron transfer (AGET) for atom transfer radical polymerization (ATRP) in miniemulsion [16]. First-order kinetics justified

that polymerization was well controlled however, kinetics of polymerization decreased by increasing the clay loading. The apparent propagation rate constant (k_{app}) of polymerization in the case of poly (styrene-co-butyl acrylate) was 4.079×10^{-6} , which becomes 0.558×10^{-6} in the case of poly (styrene-co-butyl acrylate)/clay nanocomposite having 2% nanoclay. A decrease in the polymerization rate was related to the hindrance effect of nanoclay layers on monomer diffusion toward the loci of growing macroradicals [16].

Smith-Ewart theory [17] for conventional emulsion polymerization of styrene states that the number of polymer particles (N_p) and the rate of polymerization (R_p) vary with $[\text{SDS}]^{0.6}$, but in miniemulsion polymerization, this trend was different, as the nucleation and surfactant distribution mechanisms were different. The kinetics of styrene miniemulsion polymerization in the presence of organoclay and the morphologies of water based nanoclay/styrene composite latexes had been reported by Tong [18-20] and Mirzataheri, et al [9]. Tong and coworkers [18] found that the presence of nanoclay reduces both the rate of polymerization and final conversion of styrene miniemulsion polymerization. Bon and Calver [21] found out the role of pristine nanoclay on styrene miniemulsion polymerization as a dispersant, since clay stabilized the dispersed particles without using any surfactant in their recipe. Synthesis of polystyrene/polybutyl acrylate latex and miniemulsion kinetics of the dispersion copolymerization of styrene and butyl acrylate was done by Saenz et al, either [22].

Based on surface hydrophobicity of Cloisite, less hydrophobic compounds can stabilize O/W emulsions, as hydrophobic modified particles act as stabilizer for W/O emulsions [23]. Also it was noted that armored structures for particles covered

by the clay platelets can act as super-heat barrier, therefore increase the thermal stability of polymers [24-25].

In our previous research [9], kinetics behavior of poly (styrene-co-butyl acrylate) nanocomposite latex was studied for low solid contents (up to 20%) and low clay concentration (up to 5 wt%).

In this research work, miniemulsion polymerization was used for making nanocomposites of higher solid contents (20 and 40%) water-borne poly (styrene-co-butyl acrylate) including higher amounts of Cloisite 30B (7 wt% and 10 wt%) and then, kinetical behaviors was studied.

Kinetic considerations proved miniemulsion is a reliable technique for gaining controlled morphology of platy plates of MMT within the polymer particles. To understand the role of nanoclay on particle size and polymerization rate, the nanoclay content in a series of miniemulsion recipes was varied and the resulting data were analyzed to elucidate the role of Cloisite 30B on the mechanism and parameters of polymerization rate.

It should be emphasized that although our results deals with higher clay and higher solid contents, fortunately, all latexes were stable for a long period of time. No instability, coagulation or coalescence was observed. Also by morphological studies was shown that core-shell plus Pickering structures were formed. Therefore, it is possible to control the nanoparticles morphologies without using more chemical reagents; as no one has reported yet.

2. Experimental procedure

2.1. Materials

Styrene was purified by two times washing with 5% aqueous NaOH solution (W/V) and rinsed with

distilled water. It was stored on dried CaCl_2 at 0 °C prior to use. 2, 2'-Azo-bis-isobutyronitrile (AIBN) was kept refrigerated prior to use. All other reagents were analytical grade and were used as received. Cloisite 30B, which is a natural montmorillonite modified with methyl tallow bis-2-hydroxyethyl, quaternary ammonium chloride (MT2EtOH), was purchased from Southern Clay Products Company (Gonzales, USA), with gallery d_{001} equal to 1.74.

2.2. Synthesis of copoly (styrene/ butyl acrylate)- Cloisite 30B nanocomposites

Styrene, butyl acrylate, hexadecane, and Span 80 were under magnetic stirring (300 rpm) for 60 min at room temperature and kept cool for 25 min. Then it was placed in sonicator for 20 min. Meanwhile, aqueous phase II was prepared from distilled water and Span 80 under simple stirring at room temperature for 15 min and then kept cool for 15 min. Two phases were mixed under magnetic stirring for 30 min. Then, SDS was added to the above dispersion, and further homogenization and ultrasonication was applied by the sonicator probe for 10 min. The prepared miniemulsion with solids content of 20% and 40 % including 7 and 10 wt% clay was used for subsequent polymerization (Table 1). In a four-necked 250 mm glass reactor equipped with condenser, AIBN (1.5 wt% relative to the weight of all monomers) was added and degassed by N_2 at room temperature for 20 min. Then, the set-up was placed in a water bath at 60- 65 °C and the temperature was kept constant during polymerization reaction. Polymerization was continued at this temperature for 360 min under mechanical stirring (300 rpm) in the presence of sodium bicarbonate (1 wt% relative to the weight of clay and monomers) as buffer. Finally, reaction

was terminated by adding one drop of 1% (W/V) hydroquinone solution in methanol into the latex sample. It was expected to receive random copolymer of styrene/ butyl acrylate with mostly acrylate end-tethered polymer chains (due to the monomer reactivity ratios) surrounded by clay layers. This kind of structure is so demanded for adhesive and coating production [21].

Table 1. Miniemulsion recipe of poly (styrene-co-butyl acrylate)-Cloisite 30B nanocomposite latex.

Phases	Components* (g)	(20% S.C. & 7 wt% Clay)	20% S.C. & 10 wt% Clay)	1% S.C. & 7 t% Clay)	% S.C. .0 wt% Clay)
Phase I	Styrene	12.52	12.19	25.04	14.36
	Butyl acrylate	6.17	6.00	12.34	11.00
	Cloisite 30B	1.31	1.8	2.62	3.64
	Hexadecane	1.12	1.10	2.24	2.18
	Span 80	0.1	0.1	0.1	0.1
Phase II	Water	78.48	78.51	59.6	58.42
	Span 80	0.3	0.3	0.3	0.3

*S.C. stands for solid content

2.3. Characterization

Particle size and particle size distribution (*PDI*) of miniemulsions were measured by using a laser light scattering (Zetasizer Nano ZS, Zetasizer Nano Series of Malvern instruments, UK).

Direct ultrasonication (probe immersed in the samples) was performed by 20 KHz \pm 500 Hz ultrasonic generator, SONOPULS ultrasonic homogenizer, Model HEGM 2200 from BANDELIN Electronic GmbH & Co. KG (Germany) and the used probe was a titanium microtip MS-73 with a 3 mm diameter from the above company worked at pulsed mode, and a power of 75-80%.

KERN 770 balance (densitometer) from Germany was used for measuring the density of samples with accuracy of $\pm 10^{-4}$ g.

TEM instrument model Tecnai G² from FEI Company (Netherland, Germany) at voltage of 200

kV was used which was kindly provided by the POLYMAT Institute. The samples were prepared by casting a drop of 40-50 times diluted latex solution onto a 200-mesh covered formvar/carbon coated copper grid at room temperature and dried overnight.

3. Results and discussion

Conversion variation against time has been plotted for all samples in Fig. 1.

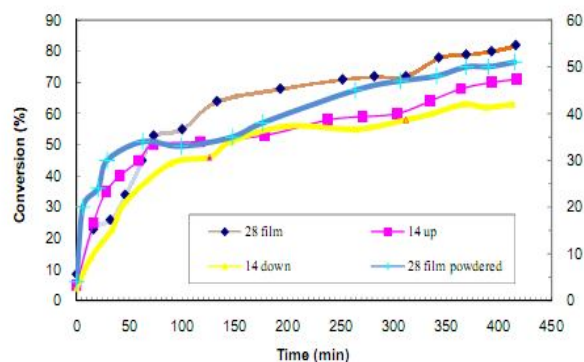


Fig. 1. Conversion versus time.

Usually, at the beginning of miniemulsion polymerization (0 min), conversions up to 10% are observed due to the high energy transfer of ultrasound irradiation. Variations in the conversion against time showed that sample 28 film has higher conversion and vice versa, sample 14 down shows lowest conversion at the same time, as the final conversion (X_f) for the nanocomposites latexes were 0.82, 0.71, 0.63 and 0.51%, respectively.

Then the reaction rates (R_p) were calculated from equation 1:

$$R_p = [M]_0 dX/dt \quad (1)$$

In which, t is the reaction time (min), $[M]_0$ is the initial monomer concentration (mol L⁻¹), X is the fractional conversion, and dX/dt was calculated from the slope of the curve drawn in Fig. 1. Therefore, the reaction rate (R_p) was plotted against time (Fig. 2) and fractional conversions

(Fig. 3), which indicate the typical miniemulsion kinetics, clearly. The maximum of R_p was obtained after about 230, 190, 130 and 98 min for samples including 10% clay, 7% clay (with 40% and 20% solid contents), respectively in Fig. 2. Obviously, these results distinguished our miniemulsion from the classical emulsion polymerization, where the maximum polymerization rate should remain constant until the gelation state [19-20].

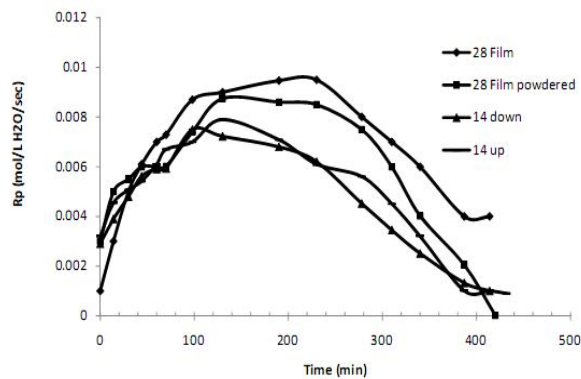


Fig. 2. Rate of polymerization (R_p) as a function of polymerization time.

Outstanding distinguish of miniemulsion polymerization with emulsion is the absence of interval II of emulsion polymerization in miniemulsion. Since the droplet nucleation is the predominating initiation mechanism in miniemulsion, causes a continuous decrease of monomer concentration and polymerization rate [25]. The polymerization rate versus reaction time (Fig. 2) and fractional conversion (Fig. 3) showed that all latex samples followed a similar kinetic behavior during miniemulsion polymerization.

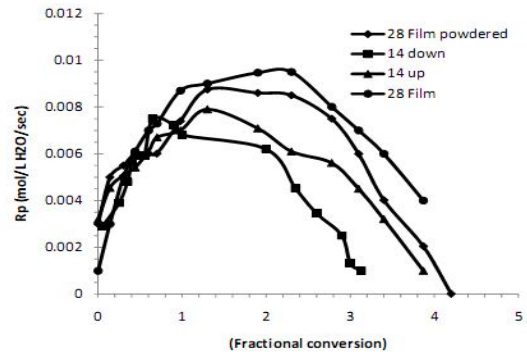


Fig. 3. Rate of polymerization (R_p) as a function of fractional conversion.

It was observed that the rate of polymerization changed by changing the clay and solid content percentages, while for sample 28 film, the highest rate and conversion was observed. By increasing the clay content up to 10% and solid content up to 40%, a continues retarding effect on the polymerization rate and the fractional conversion was found. According to Fig. 3, which is the typical miniemulsion polymerization curve, there is an increase in R_p during Interval I and then a decrease in R_p at Interval III, while a constant polymerization rate was not expectable in Interval II.

The number (N_i) of monomer droplets (N_m) or polymer particles (N_p) per liter of aqueous phase was calculated from the monomer droplet. Latex particle size was measured by dynamic light scattering which is formulated as below (Eq. 2):

$$N_i = 6 [M]_0 X_f / \pi \rho D^3 \quad (2)$$

In which, D is the volume average diameter (cm) of the polymer particle or monomer droplet, X_f is the fractional final conversion, ρ is monomer or polymer density ($g.cm^{-3}$) and $[M]_0$ is the initial monomer concentration in the aqueous phase ($g.L^{-1}$). The average number of radicals per particle (\bar{n}) at maximum R_p was found from Eq. 3:

$$\bar{n} = R_p N_A / k_p [M]_p N_p \quad (3)$$

k_p is the propagation rate constant ($L mol^{-1} s^{-1}$) in the early stage of polymerization and N_A is Avogadro's number. Value of k_p controls the kinetic of polymerization and was estimated from the initial mole fraction of monomers with regard to the data and calculations [9]. Finally, monomer concentration in the particles $[M_p]$ was expressed from this equation (Eq. 4):

$$[M]_p = \frac{1 - \chi_{R_p}}{[M]_0} \frac{1}{1 - \chi_{R_p}/\rho_m + \chi_{R_p}/\rho_p} \quad (4)$$

Where, ρ_m is the density of monomer, ρ_p is the density of the corresponding polymer and X_{Rp} is the fractional conversion at maximum rate of polymerization [9]. Maximum rate of polymerization ($R_{p(max)}$), average number of radicals per polymer particle (\bar{n}) and final conversion (X_f) have been given in Table 2 as a function of clay content and latex solid content. By increasing the solid content and clay concentration, due to the high viscosity of the monomer phase and large clay platelets, the possibility of existence of more entrapped radicals in a droplet decreased and decrease in X_f (wt%), \bar{n} and $R_{p(max)}$ was observed consequently (Table 2).

On the other hand, by increasing the clay and solid contents, degree of exfoliation has been decreased [1, 21, 26].

By increasing the clay content, exfoliation degree of clay layers was decreased and hence, these layers were hardly encapsulated inside the polymer particles and mostly were located on the surface of polymer particles. This morphology is called armored (Pickering) latex. The rest of clay had been dispersed all through the matrix without any distinguished morphology [26], except for sample 28 film [26] which showed more encapsulation degree of clay layers (Fig. 5).

Table 2. Some of kinetic results for miniemulsion polymerization.

Sample Code	Solid Cont. (%)	X_f (wt%)	\bar{n}	$R_{p(max)}$ ($mol L^{-1} H_2O sec^{-1}$)
14 down	40	0.51	0.48	0.0097
14 up	40	0.63	0.59	0.0110
28 film powdered	20	0.71	0.79	0.0156
28 film	20	0.82	0.88	0.0172

It was found (Table 3) that by increasing the nanoclay and solid contents, a remarkable increase in the number of monomer droplets, (N_m) per unit volume of water and also polymer particles (N_p) was observed, while their ratio N_p/N_m was nearly one.

Table 3. Calculated parameters during miniemulsion polymerization.

Sample Code	N_p	N_m	N_p/N_m
14 down	7.8E15	7.9E15	0.987
14 up	5.9E15	5.78E15	1.021
28 film powdered	3.1E15	3.02E15	1.026
28 film	1.9E15	2.1E15	0.905

This increase will cause a decrease in the polymer particle size, therefore partially exfoliated structures was observed for both 14 up and 14 down samples (Fig. 4).

As was shown in Table 3, N_m and N_p increased by increasing the nanoclay content, but their ratio was nearly one. This indicated that our system follows a real miniemulsion. Infact, number of particles per unit volume of water before and after miniemulsion polymerization indicated the extent of stability of miniemulsion and existence of droplet nucleation mechanism. This could be another evidence for the existence of Interval I

(droplet nucleation) during miniemulsion polymerization in the presence of nanoclay.

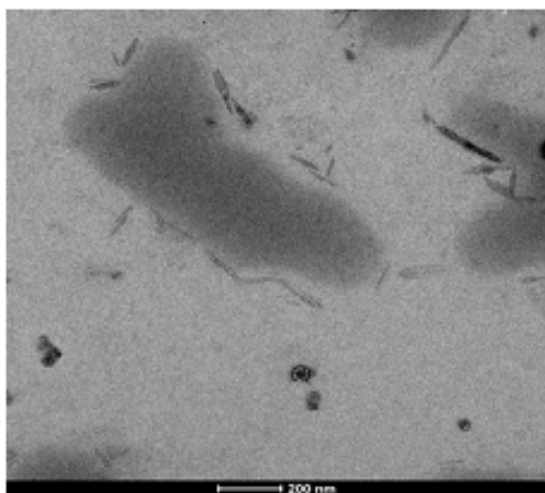


Fig. 4. TEM image for latex 14 down (scale is 200nm).

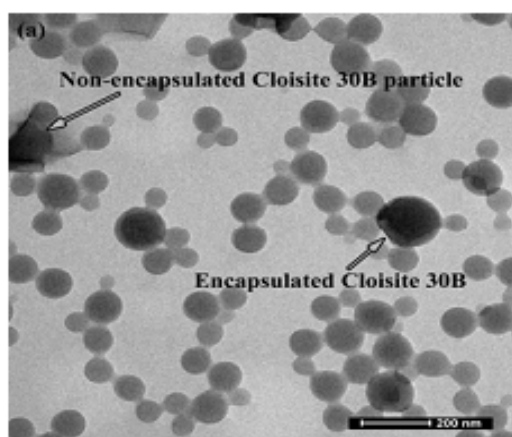


Fig. 5. TEM image for sample 28 film (scale is 200nm).

Average particle size for latex of lower solid contents was bigger than the latex particles of higher solid content. Increase in the size of polymer particles could be a sign of encapsulation. While, high amount of clay or high latex solid content had inhibited the formation of fully exfoliation structures, and fully exfoliation of clay layers was not observed for 14 down and 14 up samples.

Table 4. Diameters measured by DLS during miniemulsion polymerization.

Data [*]	14 down	14 up	28 film	28 film powdered
D_m (nm)	500	430	380	400
D_p (nm)	250	290	320	310
PDI_m	0.39	-	0.3	0.28
PDI_p	0.21	0.33	0.15	-

*the average diameter of monomer droplets (D_m) was measured at the beginning of the reaction, the average diameter of polymer particles (D_p) were measured at the end of polymerization, the polydispersity index or particle size distribution (PDI) for monomer droplets and polymer particles were all measured by DLS.

It means that some of Cloisite 30B particles were encapsulated within the polymer particles and some was located on the particles surfaces (Pickering). Hence, they were exfoliated and well dispersed throughout the nanocomposite film [26].

It seems that the higher viscosity of the monomer phase in the presence of higher percentage of organoclay decreased the rate of coupling termination and disproportionation. This conclusion could be observed from Tables 3 and 4. Therefore, the increase of \bar{n} is related to the evolution of viscosity at lower nanoclay content for the lower solid content which increases the diffusion probability of free radicals. We can say that the larger particles could keep more free radicals inside than the smaller particles. That is why a remarkable decrease in the number of polymer particles (N_p) was observed by decreasing both the solid content and clay concentration from sample 14 down towards sample 28 film. Increase in particle sizes cause more probability of radical entrapment inside the particles. The above claim can be confirmed regarding to the results obtained from Tables 2, 3 and 4. Surely, R_p has direct effect with the number of radicals per particle, clay percentage, variation in size and viscosity of medium.

Conclusion

In this research, the kinetical aspects of high solid content (20 and 40%) miniemulsion copolymerization of styrene-butyl acrylate nanocomposites of higher Cloisite 30B concentrations (7 wt% and 10 wt%) was investigated. The results proved in the presence of clay, this polymerization followed typical and real miniemulsion polymerization kinetics through droplet nucleation mechanism. Variation of X_f , R_p , N_p , N_m and \bar{n} showed that, by increasing the polymer particle size, more reactive radicals entered into the polymer particles. In this work, due to the high latex solid content and clay amounts, various morphologies were observed, for example some clay particles appeared on the surface of polymer particles. This is similar to the principle of Pickering (armored) emulsion polymerization in which the whole system is stabilized by solid particles (here is clay) and not by surfactant. However, encapsulation of nanoclay within polymer particles for 28 film and 28 film powdered was observed more significantly than the 14 up and 14 down which were of smaller size (armored was observed). Various degrees of exfoliation of MMT were confirmed for all samples, based on the obtained kinetic parameters.

Researchers proved that reduction in permeability is due to the clay content; exfoliation of clay layers and its dispersion within polymer matrix against diffusion of all permeates molecules. Observed armored latex particles suggest new barrier applications with honeycomb morphology. This honeycomb structure is well suitable for making sensitive and barrier packaging films against water and gases, which is one of the most novelties of this research work.

Acknowledgment

The financial support of this work by Iran Polymer and Petrochemical Institute (IPPI, Iran-Tehran) and advice of Prof. J. R. Leiza (POLYMAT Institute of the University of the Basque Country- Spain) is gratefully acknowledged.

References

- [1]. K. Landfester, *Annual Rev. Mater. Res.* 36 (2006) 231-79.
- [2]. K. Landfester, *Macromol. Rapid. Commun.* 22 (2001) 896-936.
- [3]. A. R., Mahdavian, Y. Sarrafi and M. Shabankareh, *Polym. Bull.* 63 (2009) 329-340.
- [4]. K. Landfester, *Macromol. Symp.* 150 (2000) 171-178.
- [5]. N. Bechthold, F. Tiarks, M. Willert, K. Landfester and M. Antonietti, *Macromol. Symp.*, 151 (2000) 549-555.
- [6]. J. Ugelstad, *Makromol. Chem.*, 179 (1978) 815-817.
- [7]. C. D. Anderson, E. D. Sudol and M. S. El-Aasser, *J. Appl. Polym. Sci.*, 90 (2003) 3987-3993.
- [8]. J. M. Asua, *Prog. Polym. Sci.*, 27 (2002) 1283-1346.
- [9] M. Mirzataheri, A. R. Mahdavian, M. Atai, *Polym. Int.*, 60 (2011) 613-619.
- [10] J. M. Asua, *Polymeric dispersion: principles and applications*, Nato ASI Series, Series E: Applied Sciences, Vol. 335, Kluwer Academic Publishers, The Netherlands (1997).
- [11] N. Greesh, R. Sanderson, and P. Hartmann, *Polymer* 53(3) (2012) 708-718.
- [12]. E. T. a. van den Dungen, J. Galineau, and P. C. Hartmann, *Macromolecular Symposia*, 313-314(1) (2012) 128-134.

- [13]. M. Abdullahi, M. A. Semsarzadeh, *European Polymer Journal*, 45 (4) (2009) 985-995.
- [14]. L. Ahmadian-Alam, V. Haddadi-Asl, H. R.-Mamaqani, L. Hatami, M. S.-Kalajahi, *J. Polym. Res.*, 19 (2012) 9773.
- [15]. L. Ahmadian-Alam, V. Haddadi-Asl, L. Hatami, H. Roghani-Mamaqani, M. Salami-Kalajahi, *Int. J. Chem. Kinet.* 44 (2012) 789–799.
- [16]. L. Hatami, V. Haddadi-Asl, L. Ahmadian-Alam, H. Roghani-Mamaqani, M. Salami-Kalajahi, *International Journal of Chemical Kinetics*, 45 (4), (2013) 221–235.
- [17]. W. V. Smith and R. H. Ewart, *J. Chem. Phys.* 16 (1948) 592-599.
- [18]. Z. Tong and Y. Deng, *Macromol. Mat. Eng.* 293 (2008) 529-537.
- [19]. Z. Tong and Y. Deng, *Ind. Eng. Chem. Res.* 45 (2006) 2641-2645.
- [20]. Z. Tong and Y. Deng, *Polymer*, 48 (2007) 4337-4343.
- [21]. S. Bon, F. Colver and J. Patrick, *Langmuir* 23 (2007) 8316-8322.
- [22]. J. M. Saenz and J. M. Asua, *Macromolecules* 31 (1998) 5215-5222.
- [23]. R. Ianchis, L. O. Cinteza, D. Donescu, C. Petcu, M. C. Corobea, R. Somoghi, M. Ghiurea, and C. Spataru, *Applied Clay Science* 52 (1–2) (2011) 96–103.
- [24]. N. Greesh, R. Sanderson, and P. Hartmann, *Polymer* 53 (3) (2012) 708–718.
- [25]. G. W. Poehlein, *Emulsion Polymerization (Overview)*, *Polymeric Materials Encyclopedia*, Vol. 3, Ed by J. C. Salamone, CRC Press Inc., Boca Raton, (1996).
- [26]. M. Mirzataheri, *J. Nanostructures* 3 (2013) 93-101.